Journal of Water & Health

IWA PUBLISHING

Journal of Water and Health Vol 21 No 5, 601 doi: 10.2166/wh.2023.298

Water treatment membranes embedded with a stable and bactericidal nanodiamond material

Abelardo Colon [a,b,*], Javier Avalos[a,c], Brad R. Weiner [a,d], Gerardo Morell [a,c] and Rafael Ríos [b]

[a] Molecular Science Research Center, University of Puerto Rico, San Juan, PR 00926, USA
[b] Department of Environmental Sciences, University of Puerto Rico, San Juan, PR 00925-2537, USA
[c] Department of Physics, University of Puerto Rico, Bayamón, PR 00959, USA
[d] Department of Chemistry, University of Puerto Rico, San Juan, PR 00925-2537, USA
*Corresponding author. E-mail: abelardo.c.olon@gmail.com

AC, 0000-0001-6969-8943; BRW, 0000-0002-5255-1918; GM, 0000-0002-5255-1918; RR, 0000-0003-4727-7309

ABSTRACT

Filtration has emerged as a critical technology to reduce waterborne diseases caused by poor water quality. Filtration technology presents key challenges, such as membrane selectivity, permeability and biofouling. Nanomaterials can offer solutions to these challenges by varying the membranes' mechanical and bactericidal properties. This research uses nanodiamond particles with facile surface functionality and biocompatibility properties that are added to membranes used for filtration treatments. Scanning and transmission electron microscopy (SEM and TEM) and Fourier transform infrared spectroscopy (FTIR) were performed to study the membrane surface. FTIR spectra confirms an increase in oxygen functional groups onto the ultradispersed diamond's (UDD) surface following acid treatment. SEM images show particle deagglomeration of functionalized UDD at the membrane surface. Tensile strength tests were done to measure the UDD mechanical properties and Coliscan membrane filtration characterization was performed to determine the filter effectiveness. Polyether sulfone (PES) and polyvinylidene (PVDF) membranes expressed a change in their yield point when UDD was incorporated into the porous matrix. A significant microorganism reduction was obtained and confirmed using t-test analysis at a 95% level of confidence. UDD-embedded membranes exhibit a significant bactericidal reduction compared to commercial membranes suggesting these membranes have the potential to enhance current membrane filtration systems.

Key words: diamond, drinking water, membrane filtration, nano, water quality

HIGHLIGHTS

- Carbon nanoparticles, embedded in organic membranes, are used for microbial removal in filtration treatment.
- The removal of pathogenic microbes by these organic membranes are enhanced by the incorporation of carbon nanoparticles on their surface, leading to enhanced water filtration treatment.
- The mechanical properties of the organic membranes embedded with carbon nanoparticles are modified, creating a membrane with higher or lower yield point depending on the membrane's symmetrical or asymmetrical structure.
- The development of these organic/carbon nanoparticle membranes has the potential to enhance their useful lifetime and reduce microbial biofouling, thereby increasing drinking water quality and quantity while reducing operational costs for filtration treatment.

GRAPHICAL ABSTRACT

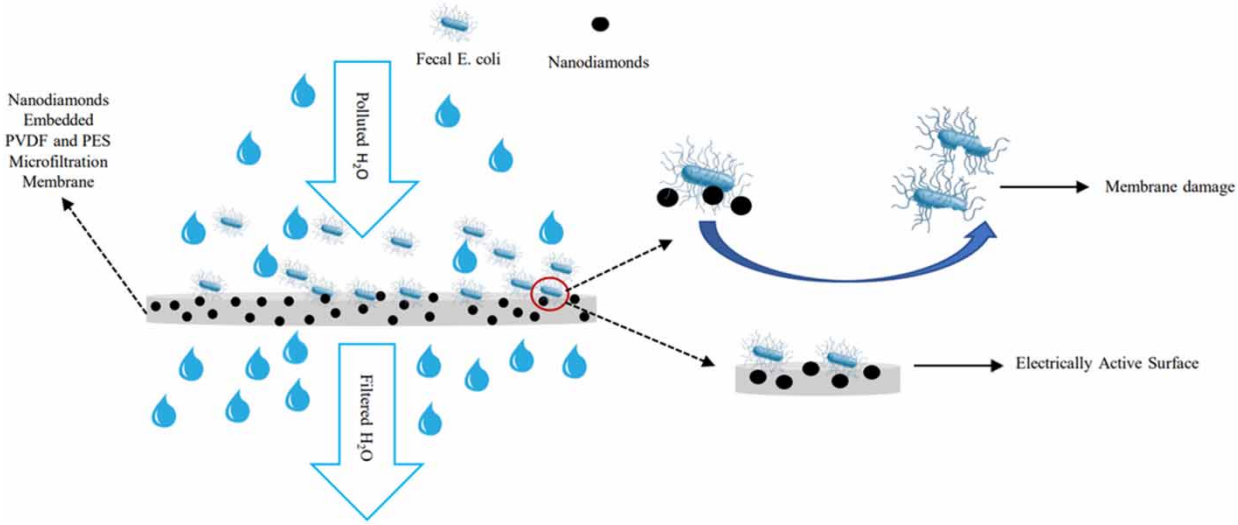

1. INTRODUCTION

With the rapidly expanding world population, exploitation of natural resources and extensive pollution, the quality and availability of potable water represent a growing threat to human health (Jackson *et al.* 2001; Ogunlela 2010; Xie *et al.* 2015); 2.2 billion people lack access to safely managed drinking water services and 297,000 children under the age of five die every year from diarrheal diseases due to poor sanitation, poor hygiene or unsafe drinking water (World Health Organization 2019). The constant expansion of impervious surfaces in urban environments is adding nonpoint source (NPS) pollutants to the watershed and groundwater catchment areas thereby changing the quality and quantity of available potable water (Sun *et al.* 2016). The recorded deterioration of public health due to waterborne outbreaks caused by this increment of impervious surfaces and improper watershed management in point catchment areas is an important issue that scientists, public health officials, politicians and community leaders need to address (Dubinsky *et al.* 2016; Kirschner *et al.* 2017).

Biocompatible applications of nano materials have been an active research area in recent years because of their unique structure and physicochemical properties. According to previous reports, nanodiamonds (NDs) in the size range 2–20 nm are biocompatible with *in vitro* human cells (Helland *et al.* 2007; Simate *et al.* 2012; Villalba *et al.* 2012) and have a large surface area leading to a high affinity for biomolecules (Solarska *et al.* 2012). Recently, ultradispersed diamonds (UDDs) have gained worldwide attention due to their inexpensive large-scale synthesis based on the detonation of carbon-containing explosives (Future Markets, Inc. 2019). These semi-crystalline nanoparticles consist of diamond nanocrystals embedded within a graphite-like carbon matrix forming large aggregates of particulates with some graphitic carbon content (Michel & Lukehart 2015; Ashek-I-Ahmed *et al.* 2019). The detonation produces UDD with a small primary particle size (ca. 4–5 nm), high biocompatibility (Schrand *et al.* 2009) and the capacity for facile functionalization. Medina *et al.* (2012) investigated the ND's surface interaction with *P. aeruginosa* Gram-negative bacteria and concluded that its bactericidal and anti-adhesive properties are due to its semiconducting properties. The electrically active surface causes membrane damage (Etemadi *et al.* 2016) and oxidative stress to the bacteria thereby inducing its death (Medina *et al.* 2012). The bactericidal properties and stability of the UDD upon usage and cleaning sparked interest in the nanoparticles for use in water treatment (Upadhyayula *et al.* 2009; Viet Quang *et al.* 2013; Yin & Deng 2015).

Membrane separation processes are increasingly utilized methods for the treatment of water and wastewater. Pressure-driven membrane technology is a common process for water purification in manufacturing and pharmaceutical industries, which need to meet water quality standards (Kumar *et al.* 2014). Currently, this methodology confronts key challenges, e.g. membrane selectivity and permeability, and fouling and membrane lifetime, all of which need to be overcome for this technology to become a leading water treatment option. Fouling resistance is one of the biggest challenges for microfiltration (MF) and nanofiltration (NF) membranes since most of them are hydrophobic. Functional nanomaterials, incorporated into

the membranes, may be the solution to these challenges by changing permeability, fouling resistance, as well as their mechanical and thermal stability (Kunduru *et al.* 2017).

Lower membrane fouling allows higher potable water productivity, less cleaning and longer membrane life, leading to reduced capital and operational costs. There are different types of membrane fouling, such as inorganic, organic and biofouling. To reduce fouling, classical solutions are available such as membrane pre-treatment, operation optimization and chemical cleaning (Beyer *et al.* 2017). Poor and ineffective pre-treatment can lead to higher rates of fouling and all of these treatments have the potential to damage the structural composition of the membrane (Sun *et al.* 2013). The chemical structure and morphology of the membrane, i.e. functional groups, charge and hydrophobicity, pore size, surface roughness and/or surface pattern are required knowledge to be able to reduce or increase fouling. The need for new cost-effective membrane materials, capable of overcoming the trade-off between anti-fouling capacity and permeability, as well as simple advanced methods of membrane modification are areas of research that need to be further understood (Qin *et al.* 2020; Zhao *et al.* 2021). The research presented here demonstrates how current water purification membranes can be enhanced by incorporating ND particles to reduce biofouling resistance problems, strengthening their mechanical stability and increasing their useful lifetime for water purification.

2. METHODOLOGY

2.1. UDD antimicrobial properties

The polluted water source used in this research was collected from the Rio Piedras River in San Juan, Puerto Rico (18°24′8.91″N, 66° 3′54.44″W), which contains high fecal bacteria concentrations (Lugo *et al.* 2011) mainly caused by anthropogenic outputs, such as household septic tanks and agricultural practices upstream of the river (Garcia-Montiel *et al.* 2014; Laureano-Rosario *et al.* 2017). A water sample of 750 cm^3 was collected and stored in a 1,000 cm^3 bottle covered in aluminum foil for low-light interaction. UDD interaction with the polluted water was obtained by mixing the UDD with 100 mL of the polluted water in a 250 cm^3 Erlenmeyer flask. Two 250 cm^3 Erlenmeyer flasks, one containing 100 cm^3 of polluted water from the river and the other with 100 cm^3 of polluted water with UDD, were placed in the incubator at 37 °C with a shaker operating at 110 RPM for UDD interaction promotion. Fecal and total coliforms bacteria analyses of the microbial polluted water were done using Coliscan Easygel petri dishes at 10-min intervals from 0 to 40 min. Bacteria colony forming units (CFU) characterization of the petri dishes was done after 24 h by using arithmetic sample mean and standard deviation analysis. The calculation of the coefficient of variation (CV) was done using sample mean and standard deviation of each time interval. Each microbial characterization was done in triplicate to reduce variability and increase precision.

2.2. UDD functionalization

UDD usage for biological applications has been limited due to its dispersibility properties caused by particle aggregation in aqueous solutions ranging from 0.1 to 1 μm in size (Stehlik *et al.* 2016; Whitlow *et al.* 2017). Recent research has demonstrated that a decrease in the degree of agglomeration is observed when pristine UDD is treated with strong acids (Pedroso-Santana *et al.* 2017).

UDD powder was obtained from Adamas Nano Inc. (Rayleigh, NC, USA) The NDs have an average aggregate size of 200 nm, a Z potential of +20 mV in deionized water (DI H_2O) and 1.7 wt.% ash content. The NDs were first sonicated with hexane to remove nonpolar impurities, followed by acetone, isopropanol and DI water to remove polar impurities. Each UDD solution was centrifuged after sonication, and the supernatant was removed. Once the UDD was cleaned, the precipitate obtained from the centrifuge was dried using Labconco FreeZone 2.5 for the lyophilization process.

The lyophilized UDD was treated with a 3:1 sulfuric acid (H_2SO_4) (CAS number 7664-93-9)/hydrogen peroxide solution 30% (H_2O_2) CAS number 7722-84-1) solution for surface functionalization and reduce particle's aggregation. The solution was heated to 120 °C for 30–40 min and then cooled to room temperature. The solution was centrifuged to separate the functionalized UDD precipitate. This process was repeated three times using nano pure water and the precipitate was dried using the Labconco FreeZone 2.5 for the lyophilization process.

Characterization of the clean UDD and functionalized UDD FTIR particles was done using a Nicolet IS 50 FT-IR Continuum IR Microscope to confirm UDD surface functional groups. The FTIR parameters used were: 32 scans in % Transmittance format with automatic atmospheric suppression. Both powders were placed in a KBr IR card with a15 mm aperture, which was inserted into the Continuum IR Microscope.

2.3. UDD membrane characterization

To investigate the interaction between UDD nanoparticles and commercial membranes, a combination of electron microscopy (JSM-7500F (JEOL, Tokyo, Japan) field-emission scanning electron microscope (FE-SEM) operated at 200 kV) and tensile strength measurements (Brookfield CT3 texture analyzer) were performed to characterize the mechanical properties, i.e. the membrane's Young Modulus (the stress the membrane can withstand without deforming), yield point (the limit of the material's elastic region before changing into its plastic region) and how the elastic and plastic regions of the membrane change upon UDD incorporation. The Young modulus value was obtained by calculating the slope of the elastic region having an R^2 value of 0.9 and the yield point resulted from the elastic region stress increase before moving towards the plastic region. Commercially available membranes, polyether sulfone (PES) and polyvinylidene (PVFD), each one with different surface morphologies and composition, were used. The PES membrane has a symmetric pore size of 0.5 μm with dimensions of 150 μm thickness and a 47 mm diameter. The PVDF membrane has an asymmetric pore size of 0.45 μm, with dimensions of 125 μm of thickness and a diameter of 47 mm. UDD-embedded membranes were fabricated by doing a dead-end filtration of 0.10 wt./vol% UDD solution in 125 mL DI water. The formed UDD paste was removed by sonicating the fabricated membrane, and then leaving the material with embedded UDDs at the membrane's surface and in its porous matrix. Three membrane samples were obtained, one with the UDD paste, another with 1 min of sonication for UDD paste removal and the third one with 2 min of sonication for UDD paste removal. SEM characterization for all samples was performed to verify the UDD presence at the surface of the membrane.

Sample preparation for the FE-SEM was performed by depositing 10 nm of gold, from a 99.999% Au target, onto the sample using the PELCO SC-7 Auto Sputter Coater. For membrane comparison, we sonicated the UDD-embedded membranes for either 1 or 2 min to remove the UDD excess formed above the membrane. Tensile strength stress vs. strain characterization was performed by cutting the studied membrane into 3×1 mm rectangles (0.125 mm thick) and placing them in Brookfield cT3 texture analyzer.

2.4. Coliscan membrane filtration characterization

Bacteriological studies between the commercially available membranes and the UDD-embedded ones were done using the Micrology Laboratories Coliscan membrane filtration method, a U.S. Environmental Protection Agency approved method for bacteria CFU enumeration (Taylor *et al.* 2015). The polluted water source used in this research was collected from the Rio Piedras river in San Juan, Puerto Rico watershed (18°24′8.91″N, 66° 3′54.44″W), which contains high fecal bacteria concentrations (Lugo *et al.* 2011) mainly caused by anthropogenic outputs, such as household septic tanks and agricultural practices upstream of the river (Garcia-Montiel *et al.* 2014; Laureano-Rosario *et al.* 2017). The water samples were collected in sterile bottles, stored in an ice cooler and tested within 4 h of collection. A 1:10 dilution was performed to the collected water using DI water to maintain the CFU enumeration within the limits specified by the Coliscan method. Plate counting was performed and *T*-test analysis of triplicate samples was done to identify fecal *E. coli* CFU changes between the membrane-filtered samples. The fecal *E. coli* death rate % comparison between the control and studied membranes was analyzed to see the reduction in CFU counting when the studied water was filtered with UDD-embedded membranes.

3. RESULTS AND DISCUSSION

3.1. UDD antimicrobial properties

A study to verify UDD antimicrobial properties was achieved by the treatment of polluted water with different UDD concentrations. Table 1 shows UDD-treated water fecal *E. coli* CFU and control polluted comparison at different time intervals. Results indicated a significant reduction of CFU when polluted water was mixed with UDD. At 0 min, the control water and UDD-treated water showed fecal *E. coli* bacteria concentrations of 950 ± 100 and 875 ± 98 Col/cm^3, respectively. After 40 min, control plates had a sample mean of $2{,}425 \pm 96$ Col/cm^3 and UDD-treated water plates had a sample mean of 150 ± 57 Col/cm^3. Fecal coliforms death rate results for each time interval showed a constant reduction of CFU as time passed.

In order to increase the fecal *E. coli* death rate, we increased the UDD concentration to 0.02 g/cm^3 and the results were similar. The CV % shown in Table 1 for 0.02 g/cm^3 UDD suggests a higher variability in UDD treated plates in comparison to untreated water as time passes. This high variability is likely due to a decrease of UDD-treated water (Col/cm^3). When the mean value approaches 0, the CV will approach infinity and is therefore sensitive to small changes in the mean. A 97%

Table 1 | Fecal *E. coli* CFU and CV % for polluted water and UDD-treated water with UDD petri dish samples

UDD (g/cm^3)	Time (min)	Sample mean untreated H_2O (Col/cm^3)	CV %	Sample mean UDD treated H_2O (Col/cm^3)	CV %	Death rate %
0.01	0	950 ± 100	1	875 ± 96	11	7
	10	1,225 ± 126	10	525 ± 95	18	58
	20	1,750 ± 129	7	500 ± 58	11	71
	30	2,175 ± 170	8	275 ± 50	18	87
	40	2,425 ± 96	4	150 ± 57	38	94
0.02	0	600 ± 0	0	300 ± 100	33	50
	10	733 ± 208	28	233 ± 58	50	68
	20	833 ± 153	18	200 ± 100	50	76
	30	1,000 ± 100	10	133 ± 58	43	87
	40	1,166 ± 58	5	33±58	117	97

death rate was achieved compared to the 94% at 0.01 g/cm^3 UDD concentration. These results demonstrate UDD's bactericidal properties suggesting the use of these nanoparticles as a disinfectant agent for water microbial treatment.

3.2. UDD particle characterization

Figure 1 shows the FTIR spectra for commercial and functionalized UDD nanoparticles. For both the commercial and functionalized UDD FTIR spectra, the broad feature near 3,400 cm^{-1} was assigned to the H–O stretching vibration. Previous reports have found that UDD adsorbs atmospheric water soon after the sample precipitate is exposed to air (Ji *et al.* 1998). Both spectra also showed the C–H stretching at 2,900 cm^{-1} and H–O–H bending vibration feature at 1,600 cm^{-1} (Bradac *et al.* 2018). Compared to commercial UDD, UDD functionalized spectra showed a more pronounced broad absorption band in the region 1,000–1,500 cm^{-1}, known as the UDD fingerprint area. This spectral region is correlated to the stretching vibration of C–C and C–O–C (Vatanpour *et al.* 2018). The absorption band around 1,100 cm^{-1} is characteristic of stretching vibrations of C–O–C of ether and/or ester functional groups (Dworak *et al.* 2014). This peak intensity change in the UDD functionalized surface composition is consistent with the insertion of oxygen functional groups following the acid treatment (Huang *et al.* 2012; Wang *et al.* 2017). As a result, the UDD surfaces are polar and more hydrophilic.

3.3. Membrane SEM images

SEM characterization was performed on commercial and modified membranes to understand the nature of the surface following UDD incorporation. Figure 2 presents the PES FE-SEM images at 20,000× magnification for surface analysis. Figure 2(a) shows the PES's symmetric porous matrix prior to the addition of the UDD solution. When UDDs were added, a cluster formation can be seen imbedded in the porous matrix (Figure 2(b)). These UDD clusters have different

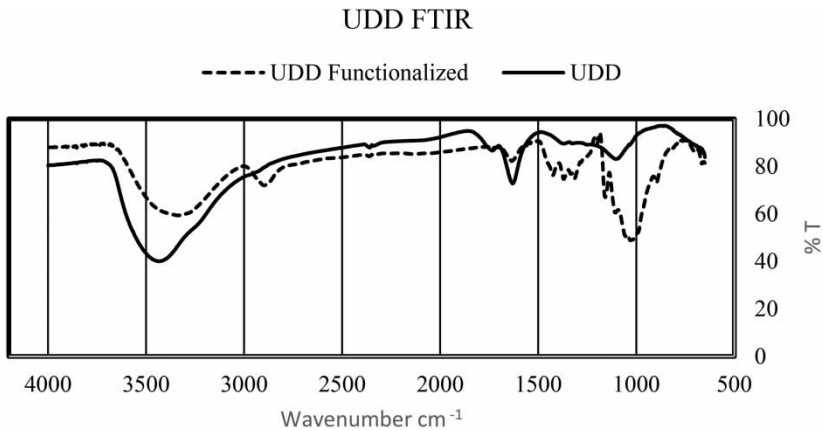

Figure 1 | FTIR spectra of pristine UDD (solid line) and UDD functionalized (dots line). The results showed typical vibration peaks for UDD and for UDD functionalized peak characteristics near 3,400 cm^{-1} (–OH stretch), 1,700 cm^{-1} (C = O stretch) and around 1,100 cm^{-1} (C–O–C stretching).

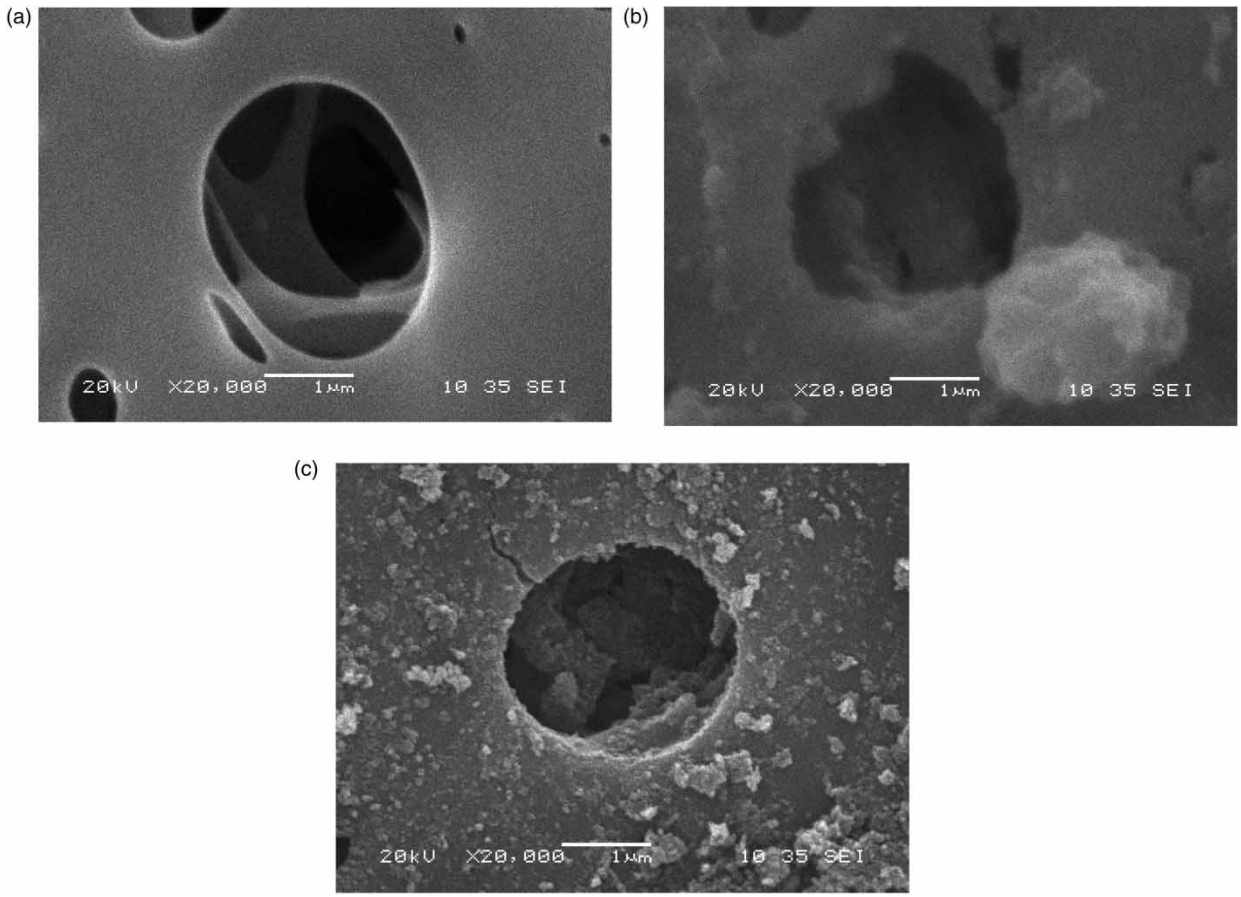

Figure 2 | FE-SEM surface porous matrix images of commercial PES (a); UDD modified PES (b); UDD functionalized PES (c). UDD PES and UDD functionalized PES membrane images show UDD particles that are present both on the membrane's surface and inside the porous structure of the membrane. The functionalized UDD membrane shows the particles to be more dispersed throughout the membrane and inside its pores.

sizes, ranging from 0.1 to 10 μm, and are most likely caused by the coupling of C–C bonds between nanoparticles (Popov 2021), van Der Waals forces and electrostatic interactions (Zheng *et al.* 2009; Wahab *et al.* 2015). Different from Figure 2(b), the embedded functionalized UDDs (Figure 2(c)) form smaller clusters within the porous matrix. The UDD amount embedded on PES membranes changes when sonication is done to remove the nanoparticles' excess above the membrane's surface. Table 2 shows how Wt.% of UDD embedded in the membrane is significantly reduced after 1 and 2 min of sonication.

Table 2 | Wt.% of UDD embedded on PES membrane

Membrane	Weight (g)	UDD Wt.%
PES	0.0696 ± 0.0001	0
UDD PES	0.1048 ± 0.0140	51
UDD PES Funct.	0.1127 ± 0.0013	62
UDD PES 1 min	0.0751 ± 0.0073	8.0
UDD PES 2 min	0.0788 ± 0.0062	13
UDD PES Funct. 1 min	0.0716 ± 0.0004	2.9
UDD PES Funct. 2 min	0.0712 ± 0.0001	2.4

For UDD PES and UDD Funct. membranes, Wt.% are 51 and 62% compared to 8.0 and 2.9%, respectively, after sonication is performed for 1 min to remove UDD excess above the membrane.

Similar to PES membranes, PVDF SEM images show UDD nanoparticles embedded at the membrane's surface. The asymmetric porous matrix of PVDF (Figure 3(a)) is covered by UDD nanoparticles when the dead-end filtration technique is performed and the UDDs are embedded (Figure 3(b) and 3(c)). The cluster size decrease shown in Figures 2(c) and 3(c) suggests that the acid treatment not only increases the oxygen-containing functional groups present in the UDDs but also deagglomerates the ND (Astuti *et al.* 2017) causing these nanoparticles to be more dispersed throughout the membrane surface and inside the porous matrix (Ushizawa *et al.* 2002; Yu *et al.* 2006; Xu & Xue 2007).

The PVDF membrane's structure also plays a role when UDDs are embedded into its porous matrix (Table 3). UDD Wt.% on UDD Funct. PVDF membranes are 27% less compared to UDD PVDF. UDD deagglomeration of clusters and the asymmetric structure of PVDF compared to the symmetric PES can be a possible reason for the UDDs to pass through the porous matrix and not be embedded above the surface.

From an operational point of view, the leaching of biocompatible nanoparticles, i.e. UDD, may be part of the sieving effect phenomena during the membrane filtration process (Drioli *et al.* 2017). The particles larger than the pore size are retained, and the smaller size nanoparticles are leached into the effluent water.

3.4. Membrane tensile strength

The membrane tensile strength characterization was performed using the STAM-D, SANTAM instrument to measure a strain vs. stress curve to determine Young Modulus and yield point values when UDDs were embedded into its porous matrix. Figure 4 presents the PES UDD tensile strength curves between the pristine UDD and functionalized UDD-embedded membranes. Figure 4(a) shows how the elastic region's yield point increases when the UDD are embedded to the membrane

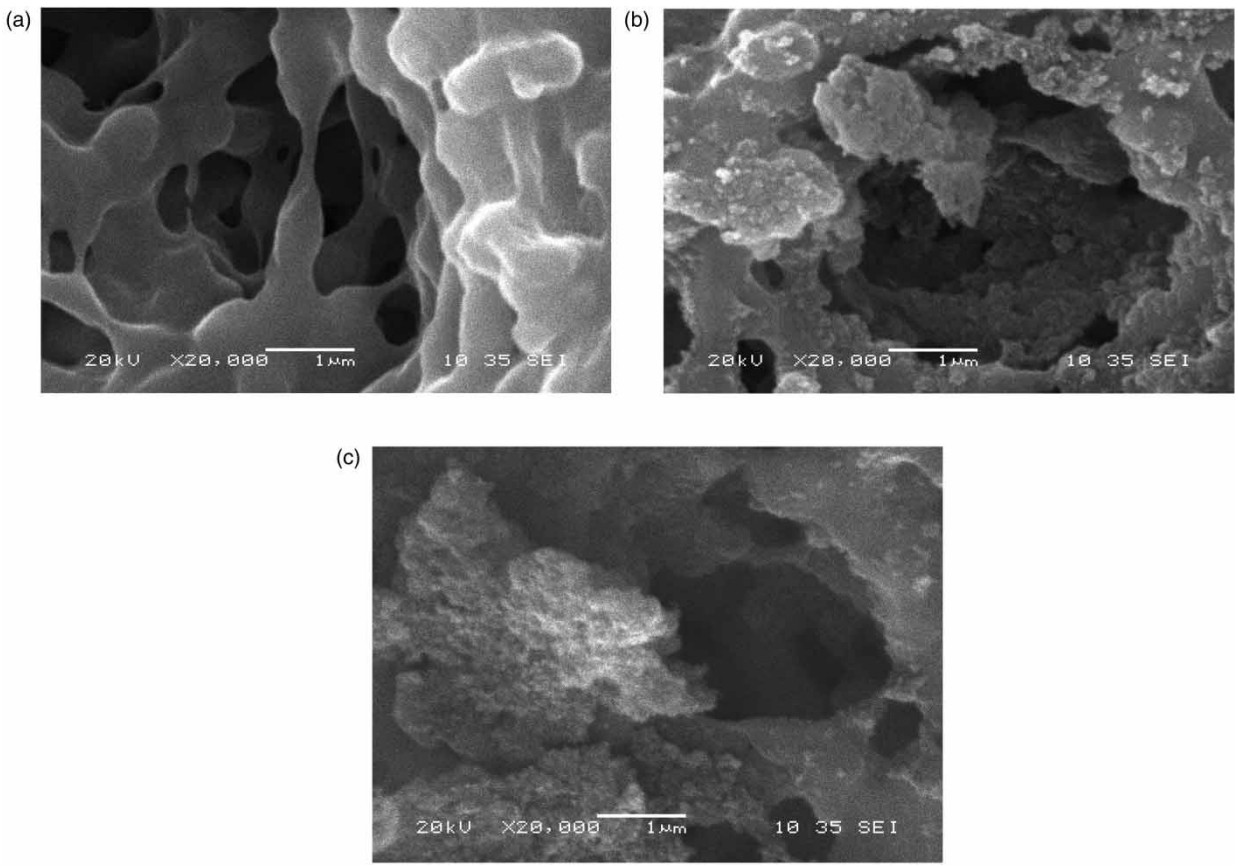

Figure 3 | SEM images for commercial PVDF (a), UDD PVDF (b), and UDD functionalized PES (c). SEM images show UDD adhesion to the PVDF membrane around and inside the membrane's pores.

Table 3 | Wt.% of UDD embedded on PES membrane

Membrane	Weight (g)	UDD Wt.%
PVDF	0.1205 ± 0.0002	0
UDD PVDF	0.1739 ± 0.0092	44
UDD PVDF Funct.	0.1413 ± 0.0084	17
UDD PVDF 1 min	0.1472 ± 0.0064	13
UDD PVDF 2 min	0.1393 ± 0.0021	16
UDD PVDF Funct. 1 min	0.1426 ± 0.0034	14
UDD PVDF Funct. 2 min	0.1430 ± 0.0010	15

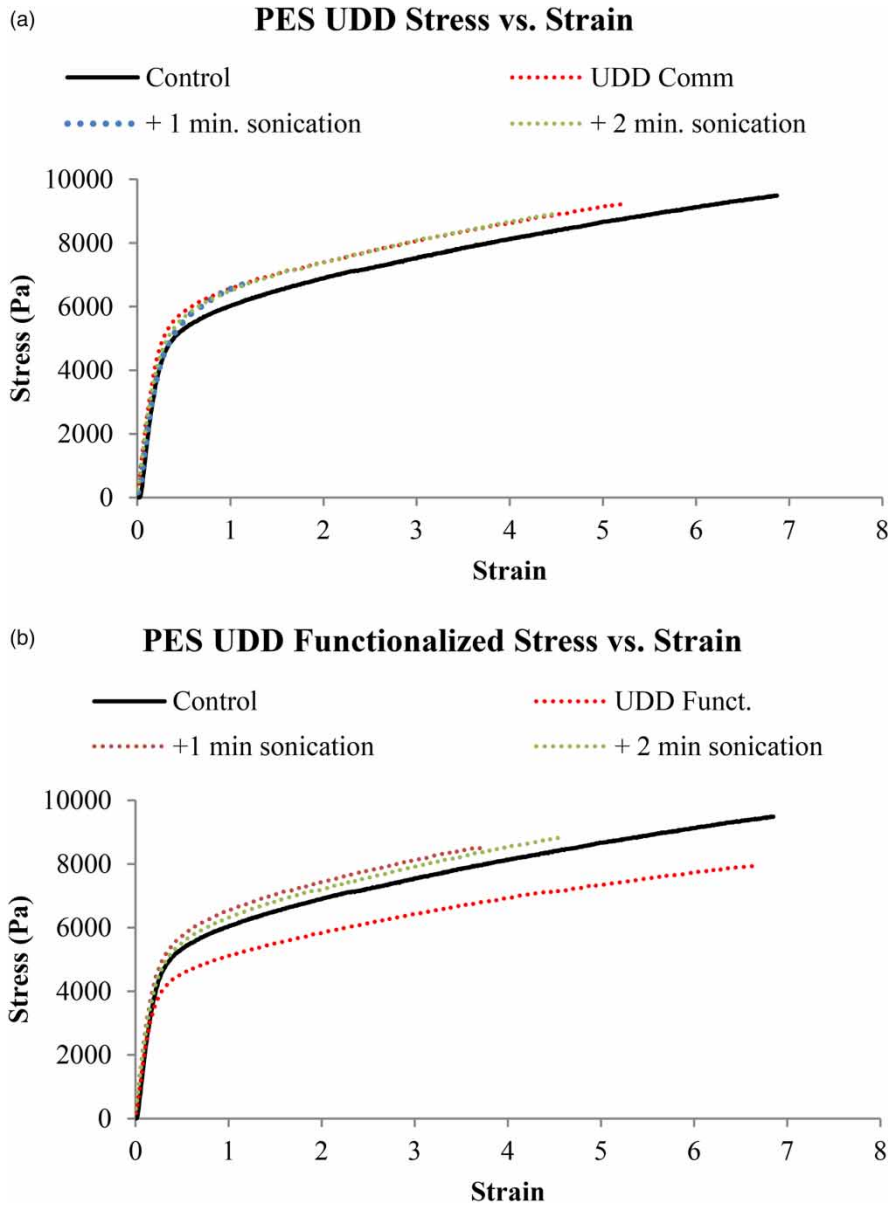

Figure 4 | PES strain vs. stress curve for PES UDD composite membrane (a) and UDD Funct. embedded PES membrane (b). Compared to commercial PES, sonicated UDD functionalized embedded PES membranes showed a higher yield point values suggesting that the NDs can increase the membrane's stress capacity in the elastic region without changing its original form.

surface and porous matrix. When functionalized UDDs are inserted in the membranes (Figure 4(b)), it also increases the membranes yield point but, after the UDD paste is removed by sonicating the membrane.

The PES membrane's ability to withstand stress without deforming between commercial PES (control) and UDD-embedded PES samples is shown in the Young Modulus (Table 4) values. The results show that PES' ability to withstand stress does not significantly change when UDD nanoparticles are embedded into the membrane's porous matrix. These findings suggest that the incorporation of UDD into the porous matrix does not change the membrane's ability to withstand stress but does increase its yield point in the elastic region, enhancing its ability to support higher stress before deformation.

For PVDF membranes, a different result was seen compared to PES. Figure 5 shows the strain vs. stress curve for PVDF (control) and UDD-embedded PVDF membranes and Table 5 shows the membranes' Young Modulus. UDD-embedded

Table 4 | Young Modulus value comparison between the pristine UDD and functionalized UDD-embedded PES membranes

Young Modulus (Pa)	PES	PES UDD	PES UDD + 1 min sonication	PES UDD + 2 min sonication
$E = \frac{\sigma}{\epsilon}$	20,878	21,271	20,120	20,505
Young Modulus (Pa)	**PES**	**PES UDD Funct.**	**PES UDD Funct. + 1 min sonication**	**PES UDD Funct. + 2 min sonication**
$E = \frac{\sigma}{\epsilon}$	20,878	21,421	20,795	19,192

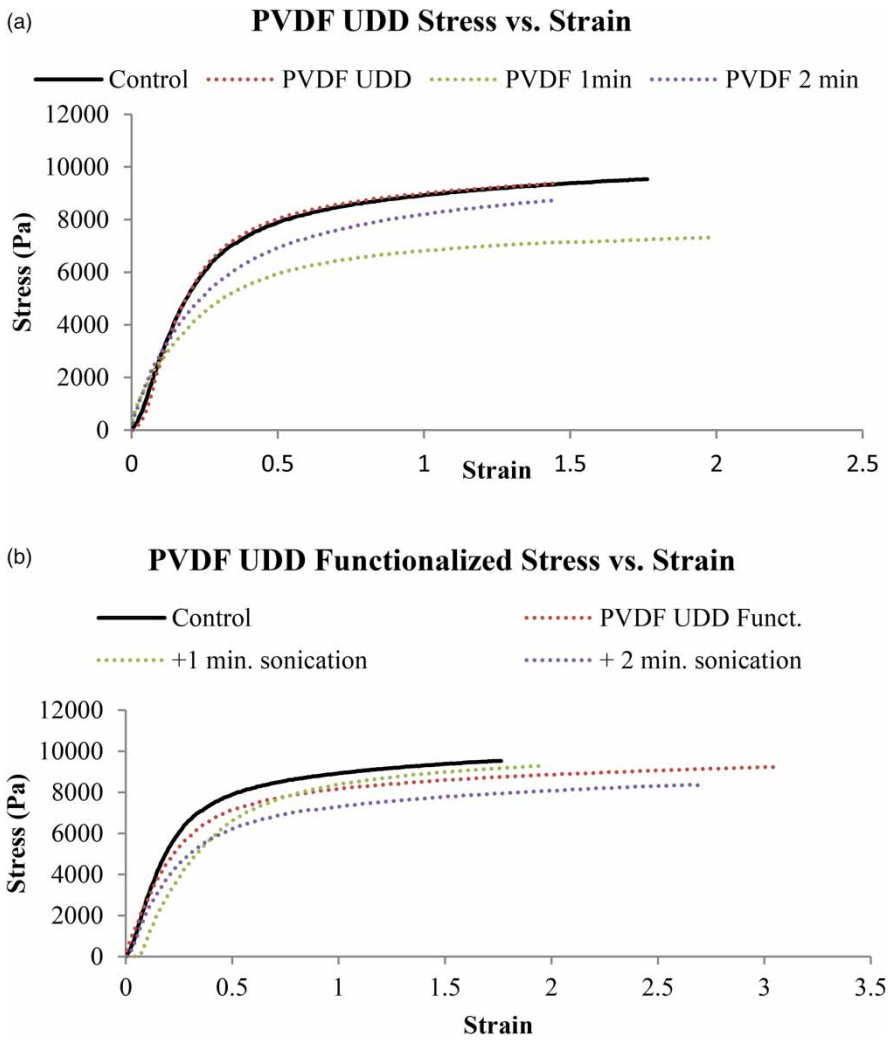

Figure 5 | Strain vs. stress curve for PVDF pristine UDD membranes (above) and PVDF UDD functionalized membranes (below).

Table 5 | Young Modulus value comparison between the pristine UDD and functionalized UDD-embedded PVDF membranes

Young Modulus (Pa)	PVDF	PVDF UDD	PVDF UDD + 1 min sonication	PVDF UDD + 2 min sonication
$E = \frac{\sigma}{\epsilon}$	27,705	29,755	21,381	23,940
Young Modulus (Pa)	**PVDF**	**PVDF UDD Funct.**	**PVDF UDD Funct. + 1 min sonication**	**PES UDD Funct. + 2 min sonication**
$E = \frac{\sigma}{\epsilon}$	27,705	21,163	23,573	21,503

membranes showed a decrease in yield point and Young Modulus values compared to commercial PVDF. The decrease in these properties, i.e. the membranes' ability to withstand stress without deforming in the elastic region, may be due to the UDDs dispersion throughout the asymmetrical porous surface (Yuan *et al.* 2020). These changes in the membranes' plastic and elastic regions are consistent with the findings reported in the literature on how the incorporation of NDs changes the membrane's mechanical properties (Zhai *et al.* 2011; Bedar *et al.* 2020a, 2020b).

3.5. Coliscan membrane filtration characterization

Bactericidal properties of studied membranes are illustrated in Tables 6 and 8 showing the CFU death rate % comparison between the commercial and UDD-embedded membranes. When microbially polluted water was filtered by the UDD-embedded PES membrane, the filtered water showed a death rate of 89% compared to the 88% shown by the commercially available PES membrane. At a 5% confidence interval, *T*-test analysis between the UDD-embedded PES and the commercial PES indicates no significant reduction on fecal *E. coli* CFU after the filtration was performed. Different from this, a significant difference in bacteria removal was seen, with a value of 0.02, between the functionalized UDD-embedded PES membrane and commercial PES indicating that the excess particle clusters above the membrane do not improve bactericidal properties and can lead to poor bacteria removal.

Like the previous analysis, UDD-embedded PES membranes that were sonicated to remove the excess of particle clusters above the membrane also showed that there is no significant difference when the water was filtered. Table 6 also shows the death rate % values when the water was filtered with sonicated funct. UDD-embedded PES membranes. Contrary to previous results, sonicating the UDD functionalized membranes enhances its bactericidal properties by significantly reducing fecal *E. coli* CFU as compared to commercial PES membranes. The incorporation of these nanoparticles into the membrane's porous matrix increases the bacterial death rate percentage by 5–8% depending on the sonication time for UDD cluster removal. *T*-test analysis of CFU values dependent on sonication time showed a *p*-value of 0.20 (Table 7) between PES

Table 6 | Fecal *E. coli* CFU and % rate percentage of UDD PES membrane filtration characterization

	Control	PES membrane	UDD/PES membrane	UDD/PES membrane 1 min sonication	UDD/PES membrane 2 min sonication	UDD funct./PES membrane	UDD funct./PES membrane 1 min sonication	UDD funct./PES membrane 2 min sonication
CFU	12,000	1,493	1,360	1,107	1,080	2,533	800	480
±	0	23	302	220	396	231	57	170
Death Rate %	0	88	89	91	91	79	93	96

Table 7 | *T*-test analysis of sonication time on PES UDD-embedded membranes

T-test	*p*-value at 95% significance
PES UDD 1 min and PES UDD 2 min	0.94
PES UDD Funct. 1 min and PES UDD Funct. 2 min	0.20

Table 8 | Fecal *E. coli* CFU and % rate percentage of UDD PVDF membrane filtration characterization

	Control	PVDF membrane	UDD/PVDF membrane	UDD-embedded PVDF membrane 1 min sonication	UDD/PVDF membrane 2 min sonication	UDD Funct./ PVDF membrane	UDD Funct./PVDF membrane 1 min sonication	UDD Funct./PVDF membrane 2 min sonication
CFU	12,000	2,400	2,000	1,173	780	333	260	547
±	0	139	283	335	255	61	85	220
Death rate %	0	80	83	90	94	97	98	95

Table 9 | *T*-test analysis of sonication time on PVDF UDD-embedded membranes

T-test	p = value at 95% significance
PVDF UDD 1 min and PES PVDF 2 min	0.24
PVDF UDD Funct. 1 min and PVDF UDD Funct. 2 min	0.14

UDD Funct. 1 min and PES UDD Funct. 2 min meaning that there is no significant difference of bacterial removal if the membrane is sonicated for 1 or 2 min.

For PVDF membranes, Table 8 shows the CFU values of UDD-embedded PVDF membranes in filtered water. Compared to the control sample, commercial and studied UDD PVDF membranes significantly reduce bacteria concentration with a death rate of 80 and 83%, respectively. *T*-test analysis from these two filtrations gave the value of 0.26 suggesting no significant difference. For UDD functionalized membrane comparison, a result of 0.0003 demonstrated that the incorporation of functionalized membranes into the PVDF porous matrix significantly reduces bacteria concentration compared to commercial ones. The insertion of a more dispersed UDD significantly improves PVDF bactericidal properties by reducing CFU by 17% more producing water with minimum bacteria CFU.

T-test analysis of CFU values dependent of sonication time showed a *p*-value of 0.14 (Table 9) between PVDF UDD Funct. 1 min and PVDF UDD Funct. 2 min meaning that there is no significant difference of bacterial removal if the membrane is sonicated for 1 or 2 min. These improvements in both membranes' bactericidal properties are consistent with the ones reported in the literature when this incorporation of carbon nanoparticles into organic membranes is done (Etemadi *et al.* 2016).

4. CONCLUSIONS

This research has demonstrated the potential use of UDD as a new disinfection material for water treatment. The results show that UDD effectively reduces fecal *E. coli* bacteria CFU concentration in polluted surface water. A death rate between 94 and 97% was observed in UDD-treated water plates depending on UDD concentration.

UDD FTIR spectra from functionalized UDD showed prominent peaks at the UDDs characteristic region (from 1,000 to 1,500 cm^{-1}) compared to commercial UDD, indicating the addition of oxygen-containing functional groups into the UDDs surface. SEM images of PES and PVDF membranes showed UDD particles at the membranes' surface and symmetric (PES) and asymmetric (PVDF) porous matrix. Compared to commercial UDD, functionalized UDD looked more spread throughout the membrane surface and UDD cluster sizes were smaller. The increase in oxygen-containing functional groups shown by the FTIR spectra promotes UDDs deagglomeration and enhances UDDs hydrophilic properties causing these nanoparticles to be more dispersed throughout the membrane surface and inside the porous matrix.

Tensile strength characterization for PES membranes demonstrated no change in its Young Modulus values and an increase in the membranes' yield point when UDDs were embedded. A higher yield point was observed when UDD nanoparticles are embedded into the porous matrix and the membrane is sonicated to remove the excess nanoparticles at the top of the surface. A decrease in tensile strength yield point was detected in UDD-embedded PES membranes that contained a high concentration of UDDs at the porous matrix. For PVDF membranes, a different result was seen compared to PES.

UDDs dispersion throughout its asymmetrical porous matrix makes the membranes less elastic, reducing its yield point and Young Modulus values. The changes in the membranes' plastic and elastic regions tailor towards the findings reported in the literature on how the incorporations of NDs change the membranes mechanical.

Coliscan membrane filtration characterization was performed for commercial and UDD-embedded membranes. The insertion of functionalized UDDs into the PES and PVDF commercial membranes significantly enhances bacteria removal by providing a better water quality, enhancing its current bactericidal properties and demonstrating the potential these membranes have to improve current water filtration technology for bacteria removal properties.

The development of these organic/carbon nanoparticle membranes has the potential to enhance current membrane lifetime usage by changing the membrane's plastic and elastic properties, enhancing microbial removal properties thereby having the potential to produce better drinking water quality and quantity for membrane filtration treatment systems.

ACKNOWLEDGEMENTS

This research project was supported by NASA Training Grant NNX15AI11H (PR Space Grant). The authors gratefully acknowledge the Molecular Science Research Center of the University of Puerto Rico, and the technical support from the Materials Characterization Center. The authors also acknowledge the undergraduate students Ms. Swizel Teneval Ms. Adneliz Cátala and Mr. Saúl Sandoval and the laboratory administrative staff Mr Jose Guzmán.

DATA AVAILABILITY STATEMENT

All relevant data are included in the paper or its Supplementary Information.

CONFLICT OF INTEREST

The authors declare there is no conflict.

REFERENCES

Ashek-I-Ahmed, Perevedentseva, E. V., Karmenyan, A. & Cheng, C.-L. 2019 Spectroscopy of nanodiamond surface: Investigation and applications. *Topics in Applied Physics*, 363–413. https://doi.org/10.1007/978-3-030-12469-4_11.

Astuti, Y., Saputra, F. D., Wuning, S., Arnelli & Bhaduri, G. 2017 Enrichment of nanodiamond surfaces with carboxyl groups for doxorubicin loading and release. *IOP Conference Series: Materials Science and Engineering* **172**, 012066. https://doi.org/10.1088/1757-899x/172/1/012066.

Bedar, A., Kumar, V., Debnath, A. K., Kumar, N. N., Jain, R., Tewari, P. K., Bindal, R. C. & Kar, S. 2020a Effect of nanodiamond size on γ-radiation resistance property of polysulfone-nanodiamond mixed-matrix membranes. *Diamond and Related Materials* **108**, 107963. https://doi.org/10.1016/j.diamond.2020.107963.

Bedar, A., Tewari, P. K., Bindal, R. C. & Kar, S. 2020b Enhancing γ-radiation resistant property of polysulfone membranes with carboxylated nanodiamond: Impact and effect of surface tunability. *Applied Surface Science* **507**, 144897. https://doi.org/10.1016/j.apsusc.2019.144897.

Beyer, F., Laurinonyte, J., Zwijnenburg, A., Stams, A. J. & Plugge, C. M. 2017 Membrane fouling and chemical cleaning in three full-scale reverse osmosis plants producing demineralized water. *Journal of Engineering* **2017**, 1–14. https://doi.org/10.1155/2017/6356751.

Bradac, C., Rastogi, I. D., Cordina, N. M., Garcia-Bennett, A. & Brown, L. J. 2018 Influence of surface composition on the colloidal stability of ultra-small detonation nanodiamonds in biological media. *Diamond and Related Materials* **83**, 38–45. https://doi.org/10.1016/j.diamond.2018.01.022.

Drioli, E., Giorno, L. & Fontananova, E. 2017 *Comprehensive Membrane Science and Engineering*. Elsevier, Oxford, UK.

Dubinsky, E. A., Butkus, S. R. & Andersen, G. L. 2016 Microbial source tracking in impaired watersheds using phylochip and machine-learning classification. *Water Research* **105**, 56–64. https://doi.org/10.1016/j.watres.2016.08.035.

Dworak, N., Wnuk, M., Zebrowski, J., Bartosz, G. & Lewinska, A. 2014 Genotoxic and mutagenic activity of diamond nanoparticles in human peripheral lymphocytes in vitro. *Carbon* **68**, 763–776. https://doi.org/10.1016/j.carbon.2013.11.067.

Etemadi, H., Yegani, R. & Babaeipour, V. 2016 Study on the reinforcing effect of nanodiamond particles on the mechanical, thermal and antibacterial properties of cellulose acetate membranes. *Diamond and Related Materials* **69**, 166–176. https://doi.org/10.1016/j.diamond.2016.08.014.

Future Markets Inc. 2019 *Market for Nanodiamonds. Nanotechnology Market Research*. Retrieved April 10, 2023, from https://www.futuremarketsinc.com/the-global-market-for-nanodiamonds-3/#prettyPhoto.

Garcia-Montiel, D. C., Verdejo-Ortiz, J. C., Santiago-Bartolomei, R., Vila-Ruiz, C. P., Santiago, L. & Melendez-Ackerman, E. 2014 Food sources and accessibility and waste disposal patterns across an urban tropical watershed: Implications for the flow of materials and energy. *Ecology and Society* **19** (1). https://doi.org/10.5751/es-06118-190137.

Helland, A., Wick, P., Koehler, A., Schmid, K. & Som, C. 2007 Reviewing the environmental and human health knowledge base of carbon nanotubes. *Environmental Health Perspectives* **115**, 1125–1131. https://doi.org/10.1016/B978-0-12-804300-4.00002-2.

Huang, H., Wang, Y., Zang, J. & Bian, L. 2012 Improvement of suspension stability and electrophoresis of nanodiamond powder by fluorination. *Applied Surface Science* **258**, 4079–4084.

Jackson, R. B., Carpenter, S. R., Dahm, C. N., Mcknight, D. M., Naiman, R. J., Postel, S. L. & Running, S. W. 2001 *Water in the Changing World*. Ecological Society of America, Washington, DC.

Ji, S., Jiang, T., Xu, K. & Li, S. 1998 FTIR study of the adsorption of water on ultradispersed diamond powder surface. *Applied Surface Science* **133** (4), 231–238. https://doi.org/10.1016/s0169-4332(98)00209-8.

Kirschner, A., Reischer, G., Jakwerth, S., Savio, D., Ixenmaier, S., Toth, E., Sommer, R., Mach, R., Linke, R., Eiler, A., Kolarevic, S. & Farnleitner, A. 2017 Multiparametric monitoring of microbial faecal pollution reveals the dominance of human contamination along the whole Danube river. *Water Research* **124**, 543–555. https://doi.org/10.1016/j.watres.2017.07.052.

Kumar, S., Ahlawat, W., Bhanjana, G., Heydarifard, S., Nazhad, M. M. & Dilbaghi, N. 2014 Nanotechnology-based water treatment strategies. *Journal of Nanoscience and Nanotechnology* **14** (3), 1838–1858.

Kunduru, K. R., Nazarkovsky, M., Farah, S., Pawar, R. P., Basu, A. & Domb, A. J. 2017 Nanotechnology for water purification: applications of nanotechnology methods in wastewater treatment. *Water Purification*, 33–74. https://doi.org/10.1016/b978-0-12-804300-4.00002-2.

Laureano-Rosario, A., Symonds, E., Rueda-Roa, D., Otis, D. & Muller-Karger, F. 2017 Environmental factors correlated with culturable enterococci concentrations in tropical recreational waters: A case study in Escambron Beach, San Juan, Puerto Rico. *International Journal of Environmental Research and Public Health* **14** (12), 1602. https://doi.org/10.3390/ijerph14121602.

Lugo, A. E., Ramos Gonzalez, O. M. & Rodriguez Pedraza, C. 2011 *The Rio Piedras Watershed and Its Surrounding Environment*. U.S. Department of Agriculture, Washington, DC, USA.

Medina, O., Nocua, J., Mendoza, F., Gomez-Moreno, R., Avalos, J., Rodríguez, C. & Morell, G. 2012 Bactericide and bacterial anti-adhesive properties of the nano crystalline diamond surface. *Diamond & Related Materials* **22**, 77–81.

Michel, J. A. & Lukehart, C. M. 2015 Partially oxidized potassium intercalate of ultradispersed diamond: A cautionary note. *Carbon* **86**, 12–14. https://doi.org/10.1016/j.carbon.2015.01.019.

Ogunlela, O. 2010 *GIS as a Tool for Microbial Risk Assessment in Watersheds*. Texas A&M University, Zachry Department of Civil Engineering.

Pedroso-Santana, S., Sarabia-Saínz, A., Fleitas-Salazar, N., Santacruz-Gómez, K., Acosta-Elías, M., Pedroza-Montero, M. & Riera, R. 2017 Deagglomeration and characterization of detonation nanodiamonds for biomedical applications. *Journal of Applied Biomedicine* **15** (1), 15–21. https://doi.org/10.1016/j.jab.2016.09.003.

Popov, V. 2021 Several aspects of application of nanodiamonds as reinforcements for metal matrix composites. *Applied Sciences* **11** (10), 4695. https://doi.org/10.3390/app11104695.

Qin, D., Huang, G., Terada, D., Jiang, H., Ito, M. M., Gibbons, A. H., Igarashi, R., Yamaguchi, D., Shirakawa, M., Sivaniah, E. & Ghalei, B. 2020 Nanodiamond mediated interfacial polymerization for high performance nanofiltration membrane. *Journal of Membrane Science* **603**, 118003. https://doi.org/10.1016/j.memsci.2020.118003.

Schrand, M., Ciftan Hens, S. A. & Shenderova, O. A. 2009 Nanodiamond particles: Properties and perspectives for bioapplications. *Critical Reviews in Solid State and Materials Sciences* **34** (1–2), 18–74.

Simate, G. S., Lyuke, S., Ndlovu, S., Heydenrych, M. & Walubita, L. 2012 Human health effects of residual carbon nanotubes and traditional water treatment chemical in drinking water. *Environmental International* **39**, 38–49.

Solarska, K., Gajewska, A., Kaczorowski, W., Bartosz, G. & Mitura, K. 2012 Effect of nanodiamond powders on the viability and production of reactive oxygen and nitrogen species by human endothelial cells. *Diamond and Related Materials* **21**, 107–113.

Stehlik, S., Varga, M., Ledinsky, M., Miliaieva, D., Kozak, H., Skakalova, V., Mangler, C., Pennycook, T. J., Meyer, J. C., Kromka, A. & Rezek, B. 2016 High-yield fabrication and properties of 1.4 nm nanodiamonds with narrow size distribution. *Scientific Reports* **6** (1). https://doi.org/10.1038/srep38419.

Sun, W., Liu, J., Chu, H. & Dong, B. 2013 Pretreatment and membrane hydrophilic modification to reduce membrane fouling. *Membranes* **3** (3), 226–241. https://doi.org/10.3390/membranes3030226.

Sun, Y., Tong, S. & Yang, Y. J. 2016 Modeling the cost-effectiveness of stormwater best management practices in an urban watershed in Las Vegas Valley. *Applied Geography* **76**, 49–61.

Taylor, A., Flatt, A., Beutel, M., Wolff, M., Brownson, K. & Stamets, P. 2015 Removal of *Escherichia coli* from synthetic stormwater using mycofiltration. *Ecological Engineering* **78**, 79–86. https://doi.org/10.1016/j.ecoleng.2014.05.016.

Upadhyayula, K. K., Deng, S. V., Mitchell, M. & Smith, G. B. 2009 Application of carbon nanotube technology for removal of contaminants in drinking water: A review. *Science of the Total Environment* **408**, 1–13.

Ushizawa, K., Sato, Y., Mitsumori, T., Machinami, T., Ueda, T. & Ando, T. 2002 Covalent immobilization of DNA on diamond and its verification by diffuse reflectance infrared spectroscopy. *Chemical Physics Letters* **351** (1–2), 105–108. https://doi.org/10.1016/s0009-2614(01)01362-8.

Vatanpour, V., Naeeni, R. S., Ghadimi, A., Karami, A. & Sadatnia, B. 2018 Effect of detonation nanodiamond on the properties and performance of polyethersulfone nanocomposite membrane. *Diamond and Related Materials* **90**, 244–255. https://doi.org/10.1016/j.diamond.2018.10.027.

Viet Quang, D., Sarawade, P. B., Jeon Jeon, S., Hoon Kim, S., Kim, J., Gyu Chai, Y. & Taik Kim, H. 2013 Effective water disinfection using silver nanoparticle containing silica beads. *Applied Surface Science* **266**, 280–287.

Villalba, P., Ram, M., Gomez, H., Bhethanabotla, V., Helms, M., Kumar, A. & Kumar, A. 2012 Cellular and in vitro toxicity of nanodiamond-polyaniline composites in mammalian and bacterial cell. *Materials Science and Engineering* **C32**, 594–598.

Wahab, Z., Foley, E. A., Pellechia, P. J., Anneaux, B. L. & Ploehn, H. J. 2015 Surface functionalization of nanodiamond with phenylphosphonate. *Journal of Colloid and Interface Science*, 301–309.

Wang, T., Handschuh, S., Qin, P., Yang, Y., Zhou, X. & Tang, Y. 2017 Enhancing the colloidal stability of detonation synthesized diamond particles in aqueous solutions by absorbing organic mono-, bi, and tridentate molecules. *Journal of Colloid and Interface Science* **499**, 102–109.

Whitlow, J., Pacelli, S. & Paul, A. 2017 Multifunctional nanodiamonds in regenerative medicine: Recent advances and future directions. *Journal of Controlled Release* **261**, 62–86. https://doi.org/10.1016/j.jconrel.2017.05.033.

World Health Organization 2019 *Drinking Water*. World Health Organization. Available from: https://www.who.int/news-room/fact-sheets/detail/drinking-water.

Xie, H., Yao, G. & Liu, G. 2015 Spatial evaluation of the ecological importance based on GIS for environmental management: A case study in Xingguo county of China. *Ecological Indicators* **51**, 3–12.

Xu, K. & Xue, Q. 2007 Deaggregation of ultradispersed diamond from explosive detonation by a graphitization–oxidation method and by hydroiodic acid treatment. *Diamond and Related Materials* **16** (2), 277–282. https://doi.org/10.1016/j.diamond.2006.06.006.

Yin, J. & Deng, B. 2015 Polymer-matrix nano composite membranes for water treatment. *Journal of Membrane Science* **479**, 256–275.

Yu, Q., Kim, Y. J. & Ma, H. 2006 Plasma treatment of diamond nanoparticles for dispersion improvement in water. *Applied Physics Letters* **88** (23), 231503. https://doi.org/10.1063/1.2208279.

Yuan, X. T., Xu, C. X., Geng, H. Z., Ji, Q., Wang, L., He, B., Jiang, Y., Kong, J. & Li, J. 2020 Multifunctional PVDF/CNT/GO mixed matrix membranes for ultrafiltration and fouling detection. *Journal of Hazardous Materials* **384**, 120978. https://doi.org/10.1016/j.jhazmat.2019.120978.

Zhai, Y.-J., Wang, Z.-C., Huang, W., Huang, J.-J., Wang, Y.-Y. & Zhao, Y.-Q. 2011 Improved mechanical properties of epoxy reinforced by low content nanodiamond powder. *Materials Science and Engineering: A* **528** (24), 7295–7300. https://doi.org/10.1016/j.msea.2011.06.053.

Zhao, S., Mao, C., Wang, T., Tian, X., Qiao, Z., Wang, Z. & Wang, J. 2021 High-flux polyamide thin film nanofiltration membrane incorporated with metal-induced ordered microporous polymers. *Separation and Purification Technology* **256**, 117817. https://doi.org/10.1016/j.seppur.2020.117817.

Zheng, W.-W., Hsieh, Y.-H., Chiu, Y.-C., Cai, S.-J., Cheng, C.-L. & Chen, C. 2009 Organic functionalization of ultradispersed nanodiamond: Synthesis and applications. *Journal of Materials Chemistry* **19** (44), 8432. https://doi.org/10.1039/b904302k.

First received 7 November 2022; accepted in revised form 25 March 2023. Available online 6 April 2023